

EPR spectra and linewidths of Mn^{2+} in calcite*

G. E. Barberis,[†] R. Calvo,[†] H. G. Maldonado, and C. E. Zarate

Departamento de Física, Facultad de Ciencias Exactas y Naturales, Universidad de Buenos Aires, Ciudad Universitaria, Buenos Aires, Argentina

(Received 23 September 1974)

The constants corresponding to the spin-Hamiltonian terms without cylindrical symmetry for Mn^{2+} in calcite ($CaCO_3$) have been measured by EPR techniques; it is shown that the principal axes of the spin Hamiltonian are rotated 15.5° from the crystal axes. This value allows us to obtain information about the charge distribution of the carbonate ligands. Our result is in agreement with the predictions of a simple covalent model for the carbonates. We measured also the angular variation of the linewidth of an EPR transition; our data allow us to explain the source of the inhomogeneous broadening for Mn^{2+} in our sample as random internal stresses. We compare our results with previous data obtained for Mn^{2+} in $CaWO_4$ where the source of broadening is a distribution of point defects in the sample. A method for finding the source of inhomogeneous broadening in sites of low symmetry is discussed.

I. INTRODUCTION

The electron-paramagnetic-resonance (EPR) spectra of Mn^{2+} impurities in calcite ($CaCO_3$) have been studied by many authors.¹⁻⁷ Good natural single crystals with low concentration of manganese impurities are easily found; they have a narrow EPR spectrum very appropriate for precise measurements.

It was shown by Kikuchi and Matarrese⁴ that the point symmetry at the Ca^{2+} site in calcite (and that of the substitutional Mn^{2+} impurities) is S_6 , with two inequivalent sites per unit cell which can be related by a C_2' operation. The spin Hamiltonian referred to the crystalline axes (z parallel to the c crystal axis and y parallel to the C_2' axis) can be written as

$$\mathcal{H} = \mu_B \vec{H} \cdot \vec{g} \cdot \vec{S} + A_2^0 e_2^0(\vec{S}) + A_4^0 e_4^0(\vec{S}) + A_4^3(c) e_4^3(\vec{S}) \pm A_4^3(s) s_4^3(\vec{S}) + \vec{I} \cdot \vec{A} \cdot \vec{S}, \quad (1)$$

where the first contribution is the Zeeman interaction, with μ_B the Bohr magneton; the following four terms give the zero-field splitting of the Mn^{2+} ions and the last term is the hyperfine interaction with the nuclear spin $I = \frac{5}{2}$ of the 100% abundant ^{55}Mn isotope. Higher-order Zeeman and hyperfine contributions, which are not important to fit the EPR-allowed transitions, are not included in Eq. (1). The $e_n^m(\vec{S})$ and $s_n^m(\vec{S})$ are normalized spin operators equivalent to those defined by Prather,⁸ acting on the spin $S = \frac{5}{2}$ of the Mn^{2+} ions; they are defined in Appendix A. The double sign in the $s_4^3(\vec{S})$ term of Eq. (1) takes into account the two inequivalent ions in the unit cell.

The operators $e_n^m(\vec{S})$ are real and the $s_n^m(\vec{S})$ are Hermitic, and therefore the coefficients $A_n^m(c)$ and $A_n^m(s)$ are real.

The parameters \vec{g} , \vec{A} , A_2^0 , and A_4^0 had been measured previously but there were no values for $A_4^3(c)$ and $A_4^3(s)$, even though their importance could be inferred from the splitting of the lines corresponding to the two inequivalent sites.

One of the purposes of this work is the measurement of the parameters $A_4^3(c)$ and $A_4^3(s)$; their values give important information about the role played in the crystalline electric field by the oxygen ligands and about the electronic distribution of the carbonates. In fact, the point symmetry at the Ca^{2+} sites would be D_{3d} if the calcium and carbon ions in the lattice were the only ones that contributed to the crystalline field.⁹ The oxygen ions of the carbonates reduce this symmetry to S_6 and introduce the contribution $A_4^3(s)s_4^3(\vec{S})$ to the spin Hamiltonian of Eq. (1). The effect of this term is to make the principal axes of the spin Hamiltonian different from those of the crystal; the angle of rotation can be measured and used to obtain information about the electronic distribution of the carbonate ligands.

We report here measurements of $A_4^3(c)$ and $A_4^3(s)$ and using these values we determine the principal axes of the crystalline electric field acting on the Mn^{2+} ions in calcite. These values are discussed in terms of a model for the crystalline electric field and the covalent bond of the carbonates.

Measurements of the angular variation of the EPR linewidths of Mn^{2+} in calcite are also reported in this paper. Our data are compared with the angular dependence predicted by the point symmetry of the magnetic ion. Important differ-

ences are observed when the behavior of the linewidths of this system is compared with that reported previously by us¹⁰ for Mn^{2+} in $CaWO_4$. These differences allow us to explain the sources of the inhomogeneous broadening in each case. We show how the measurement of the angular variation of the linewidths can be used to study the origin of the broadening for magnetic ions in sites of low symmetry.

II. THEORY AND CALCULATIONS

A. Position of the EPR lines

The most important contribution to the Hamiltonian of Eq. (1) is the electronic Zeeman term so that, to study the angular variations of the EPR spectra, it is convenient to choose the direction of the magnetic field as the quantization axis. Considering that the \vec{g} and \vec{A} tensors are isotropic within experimental accuracy,¹ the spin-Hamiltonian of Eq. (1) can be written as

$$\mathcal{H} = g\mu_B H S_z + A[S_z I_z + \frac{1}{2}(I_+ S_- + I_- S_+)] + A_2^0 \times \frac{1}{2} (3 \cos^2 \theta - 1) \mathcal{C}_2^0(\vec{S}) + A_2^0 \times \frac{3}{2} \sin 2\theta \mathcal{C}_2^1(\vec{S}) - A_2^0 \times \frac{3}{2} \sin^2 \theta \mathcal{C}_2^2(\vec{S}) + \{A_4^0 \times \frac{1}{8} (35 \cos^4 \theta - 30 \cos^2 \theta + 3) + \frac{1}{4} \sqrt{70} \sin^3 \theta \cos \theta [A_4^3(c) \cos 3\phi \pm A_4^3(s) \sin 3\phi]\} \mathcal{C}_4^0(\vec{S}). \quad (2)$$

The fourth-order nondiagonal spin operators have been neglected; this approximation will be discussed later in the paper. The angles θ and ϕ in Eq. (2) give the orientation of the magnetic field referred to the crystal axes.

The eigenvalues of Eq. (2) are functions of the field H and the angles θ and ϕ determined by the values of the parameters of the spin Hamiltonian,

$$E_n = E_n(g, A, A_n^m, (H, \theta, \phi)).$$

These functions are invariant to any change in the direction of the magnetic field corresponding to an operation of the S_6 point group. Then $E_n(\theta, \phi)$ transforms like the completely symmetric irreducible representation Γ_1 of S_6 . Using the transformation rules of the tesseral harmonics in S_6 ,⁸ the angular variation of the position of any

EPR transition is given by

$$g\mu_B H_{\text{trans}}(i) = k_0^0(i) + k_2^0(i) \mathcal{C}_2^0(\theta, \phi) + k_4^0(i) \mathcal{C}_4^0(\theta, \phi) + k_4^{3c}(i) \mathcal{C}_4^3(\theta, \phi) + k_4^{3s}(i) \mathcal{S}_4^3(\theta, \phi), \quad (3)$$

where the $k_n^m(i)$ are constants to be determined experimentally.

Sixth- and higher-order terms transforming like Γ_1 in S_6 could also be considered in Eq. (3) as contributions to the angular variation coming from higher-order perturbation corrections to the energy levels, due to the nondiagonal terms of the fourth-order spin Hamiltonian of Eq. (2). If only the diagonal contributions are considered, the fields of the EPR allowed transitions of the type $(S_z, I_z) \rightarrow (S_z - 1, I_z)$, are given by

$$g\mu_B H_{\text{trans}}(S_z I_z \rightarrow S_z - 1, I_z) = g\mu_B H_0 - A I_z - A_2^0 [\mathcal{C}_2^0(S_z) - \mathcal{C}_2^0(S_z - 1)] \frac{1}{2} (3 \cos^2 \theta - 1) - \{ A_4^0 [\frac{1}{8} (35 \cos^4 \theta - 30 \cos^2 \theta + 3)] - \frac{1}{4} \sqrt{70} \sin^3 \theta \cos \theta [A_4^3(c) \cos 3\phi \pm A_4^3(s) \sin 3\phi] \} \times [\mathcal{C}_4^0(S_z) - \mathcal{C}_4^0(S_z - 1)], \quad (4)$$

where S_z and I_z are the quantum numbers giving the projection of the electronic and nuclear spin along the direction of the magnetic field. It is known¹ that $g = 2.0018$, $A = 87.82 \times 10^{-4} \text{ cm}^{-1}$, $A_2^0 = -50.54 \times 10^{-4} \text{ cm}^{-1}$, and $A_4^0 = -0.0797 \times 10^{-4} \text{ cm}^{-1}$ at room temperature.

If higher-order contributions of the spin Hamiltonian of Eq. (2) are considered, changes are introduced in Eq. (4). It is easy to estimate that terms depending only in θ contribute at most 20 G to the line position of the EPR lines at X band. Assuming that $A_4^3(c)$ and $A_4^3(s)$ are of the same order of magnitude or smaller than A_4^0 , terms depending on θ and ϕ simultaneously show at

most changes of 0.1 G. These corrections are unimportant for our purposes.

The parameters $A_4^3(c)$ and $A_4^3(s)$ give contributions to the line positions depending on ϕ ; these contributions are zero for $\theta = 0^\circ$ and for $\theta = 90^\circ$ and have a maximum ϕ dependence for $\theta = 60^\circ$. It is of interest then to rotate the magnetic field in a cone with $\theta = 60^\circ$ around the c crystal axis; if both, θ and ϕ were changed during the experiment, the θ dependence of the position, which is much stronger, will mask the ϕ dependence and the error due to the indetermination of θ would be comparable to the contribution of $A_4^3(c)$ and $A_4^3(s)$. For $\theta = 60^\circ$, Eq. (4) can be written

$$H_{\text{trans}}(S_z, I_z \rightarrow S_z - 1, I_z) = K(S_z, \theta) + \left\{ -\frac{1}{4}\sqrt{70} \sin^3\theta \cos\theta [A_4^3(c) \cos 3\phi \pm A_4^3(s) \sin 3\phi] [C_4^0(S_z) - C_4^0(S_z - 1)] \right\}. \quad (5)$$

The term $A_4^3(s) \sin 3\phi$ reflects the noncoincidence of the principal axes of the spin Hamiltonian (magnetic axes) with those of the crystal. This can be easily seen if Eq. (5) is written as

$$H_{\text{trans}} = K(S_z, \theta) - \frac{1}{4}\sqrt{70} \sin^3\theta \cos\theta A_4^3(c) \cos 3(\phi \mp \alpha) \times [C_4^0(S_z) - C_4^0(S_z - 1)], \quad (6)$$

where

$$A_4^3(c) = \{ [A_4^3(c)]^2 + [A_4^3(s)]^2 \}^{1/2}$$

and

$$\tan 3\alpha = A_4^3(s)/A_4^3(c).$$

Equation (6) predicts a variation of each line with an extremum for $\phi = \pm\alpha$ when θ remains constant; if the position of a pair of lines corresponding to the same transition but different sites is plotted as a function of ϕ , the distance between the extrema gives 2α .

B. Linewidths of EPR transitions

The line shapes and linewidths of inhomogeneously broadened lines depend on the distribution and kind of defects which produce the broadening; they can be analyzed in terms of specific models of the source and several papers exist in the literature analyzing the problem.¹¹⁻¹⁶ It has been shown that different kinds of defects produce different line shapes,^{15,16} and Lorentzian, Gaussian, but mostly mixed shapes have been observed and discussed. The theories predict the behavior for given sources of broadening but in general it is difficult or impossible to check the adequacy of the models for the different systems studied experimentally.

Some information can be gained by measuring the angular variation of the linewidths. The function which describes this variation is invariant to the symmetry operations of the point group of the source of the broadening and then should transform like the completely symmetric irreducible representation of this group. The measurement of this angular variation gives then directly the symmetry of the source; it can be the same or higher than the point symmetry of the magnetic ion; randomly distributed defects of any kind cannot have a symmetry lower than that. For a cubic point symmetry, for example, the angular variation of the linewidth has to be cubic because no higher point symmetry exists. If the crystalline point symmetry is S_6 , as in the case of Mn^{2+} in calcite, the point symmetry of the source of broadening could be S_6 or any group which con-

tains S_6 as a subgroup (O_h , T_h , D_{6h} , D_{3d} , etc.). If the symmetry of the source of broadening is S_6 the angular variation of the linewidth is given by

$$\begin{aligned} \Delta H &= a + b C_2^0(\theta, \phi) + c C_4^0(\theta, \phi) + d C_4^3(\theta, \phi) + e S_4^3(\theta, \phi) \\ &= A_1 + A_2 \cos^4\theta + A_3 \cos^2\theta + B \sin^3\theta \cos\theta \cos 3(\phi \mp \beta), \end{aligned} \quad (7)$$

where θ and ϕ are referred to the crystalline axes and the two signs in β indicate the two non-equivalent sites of Mn^{2+} in calcite, as in Eq. (6) for the angle α .

In a previous paper¹⁰ we have studied the angular variation of the linewidth of Mn^{2+} in $CaWO_4$. In that case, using the properties of the S_4 point group of Mn^{2+} in the $CaWO_4$ lattice, we obtained

$$\Delta H = A_1' + A_2' \cos^4\theta + A_3' \cos^2\theta + B' \sin^4\theta \cos 4(\phi + \beta'), \quad (8)$$

where the sign of β' holds, because the two sites of Ca^{2+} in the unit cell of $CaWO_4$ are not distinguishable in EPR experiments.

In Eqs. (7) and (8) for Mn^{2+} in $CaCO_3$ and in $CaWO_4$ we assumed that the point symmetry of the sources of broadening is the same as that of the crystalline electric field. However, for Mn^{2+} in $CaWO_4$ we measured $\beta' = 0$ in Eq. (8), indicating a tetragonal point symmetry higher than S_4 (D_{2d} , D_{4h} , D_4 , or C_{4v}) for the broadening. We understand now that this experimental result indicates that the main source of inhomogeneous broadening are point defects at the position of the calcium or tungstate ions in the $CaWO_4$ lattice, but not at the oxygen sites. That is because the point symmetry around a calcium ion is D_{2d} if only calcium and tungstate ligands are considered but it is lowered to S_4 when the effect of the oxygens is considered.

III. EXPERIMENTAL TECHNIQUES AND RESULTS

The measurements were performed with an X-band EPR spectrometer, a rectangular TE_{101} cavity and a 12-in. rotating magnet. The cavity has a goniometer which allows rotation of the sample around an axis contained in the plane of rotation of the magnetic field. The c crystal direction of the calcite sample was oriented within 1° along the axis of the goniometer rod by Laue techniques. We placed the magnetic field at $\theta = 60^\circ$ from the c axis by rotating the magnet and then we change the angle ϕ with the goniometer. Because of the error in the orientation of the

sample, small changes of the angle θ are produced when the goniometer is rotated and the experimental points have to be corrected. We show in Appendix B how this correction was done.

The experimental values for the position of the transitions $S_z = -\frac{5}{2} \leftrightarrow -\frac{3}{2}$ with $I_z = -\frac{5}{2}$ corresponding to the two inequivalent sites are shown in Fig. 1. The intersection of the cone where the magnetic field moves, with the xz plane of the crystal, can be determined easily because both sites are equivalent for the magnetic field H at this angle and the EPR lines are superimposed. Two crossings differing by 60° are found, however, and we do not know which one corresponds to the xz plane of each site. For this reason the sign of α defined in Eq. (6) cannot be determined. A least-square analysis of the curves in Fig. 1 gives, when compared to Eq. (6),

$$H(G) = K_0 + 9.83 \cos 3(\phi \pm 15.5^\circ), \quad (9)$$

where $K_0 = 2908$ G. Two sets of values for the spin-Hamiltonian parameters can be proposed using our experimental data; comparing Eq. (9) with Eq. (6), we obtain

$$A_4^3(c) = (0.245 \pm 0.004) \times 10^{-4} \text{ cm}^{-1},$$

$$A_4^3(s) = \pm (0.232 \pm 0.004) \times 10^{-4} \text{ cm}^{-1},$$

or

$$A_4^3 = (0.338 \pm 0.006) \times 10^{-4} \text{ cm}^{-1}$$

and

$$\alpha = (\mp 15.5 \pm 1.0)^\circ$$

at 300°K .

The linewidths measured for the same EPR transition and the two inequivalent sites for $\theta = 60^\circ$ are shown in Fig. 2 as a function of ϕ . The labels "site 1" and "site 2" used in Figs. 1 and 2 indicate which line of Fig. 1 corresponds to each line in Fig. 2 but they do not make clear which one corresponds to each nonequivalent site in the unit cell of calcite.

At least-square analysis of the curves in Fig. 2 gives for the angular variation of the linewidths,

$$\Delta H(G) = 1.78 - 0.15 \cos 3(\phi \pm 16.4^\circ). \quad (10)$$

Comparing Eq. (10) with Eq. (7), we obtain

$$A_1 + \frac{1}{16} A_2 + \frac{1}{4} A_3 = 1.78 \text{ G},$$

$$\frac{3}{16} \sqrt{3} B = -0.15 \text{ G},$$

and

$$\beta = (\mp 16.4 \pm 1.0)^\circ.$$

The linewidths of the $S_z = -\frac{1}{2} \leftrightarrow \frac{1}{2}$ transitions are less than 1 G and isotropic within experimental

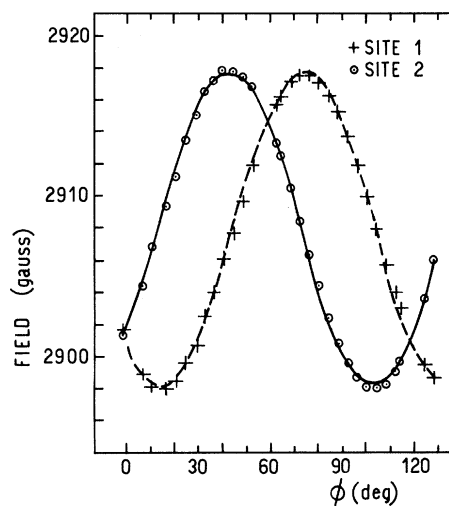


FIG. 1. Angular variation of the magnetic-field position of the EPR transition $S_z = -\frac{5}{2} \leftrightarrow -\frac{3}{2}$ with $I_z = -\frac{5}{2}$ in the cone with $\theta = 60^\circ$, as a function of ϕ . The lines were obtained by a least-square fit of the experimental data with Eq. (6).

error; those of the $S_z = \pm \frac{1}{2} \leftrightarrow \pm \frac{3}{2}$ transitions are slightly broader and anisotropic.

The values given in Fig. 2 were taken at 300°K ; they show only minor variations when our sample is cooled to 77°K .

IV. DISCUSSION

A. Spin-Hamiltonian parameters

The values of the spin-Hamiltonian parameters of an S-state ion like Mn^{2+} in diamagnetic hosts depend in a complicated way, and through high-order perturbation mechanisms, on the crystalline electric field at the position of the magnetic ion, the spin-orbit, spin-spin, and other relativistic interactions.¹⁷ No theory satisfactorily explains the enormous amount of experimental data existing for these ions; these data are then of little use, in general, to obtain detailed information about the ion or the crystal host.

We show in Sec. II that for the S_6 point symmetry of Mn^{2+} in calcite, a spin operator transforming like $\mathcal{C}_4^3(\theta, \phi')$, with ϕ' related to the angle ϕ with the crystalline axis by $\phi' = \phi - \alpha$, contributes to the spin Hamiltonian. Our experimental value of α can be used to obtain directly the charge distribution of the ligands, if the following hypotheses are made:

(i) The angle α , which relates the principal axes of the spin Hamiltonian with the crystal axes, is a characteristic of the crystalline electric field; this is equivalent to stating that the values of the constants $A_4^3(c)$ and $A_4^3(s)$ of the spin Hamiltonian of Eq. (1) are due to the same interactions and the same mechanisms. We assume in the

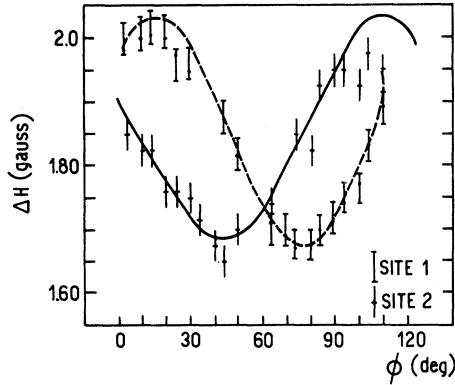


FIG. 2. Angular variation of the linewidth of the EPR transition $S_z = -\frac{5}{2} \rightarrow -\frac{3}{2}$ with $I_z = -\frac{5}{2}$, in the cone with $\theta = 60^\circ$, as a function of ϕ . The lines were obtained by a least-square fit of the experimental data with Eq. (7).

calculation that the spin-Hamiltonian parameters $A_4^3(c)$ and $A_4^3(s)$ depend linearly on the crystalline field, a fact verified in uniaxial stress experiments¹⁴ for small induced crystalline fields.

(ii) The bond of the manganese ion in the calcite crystal is ionic and so the charge of the carbonate ions is $-2e$.

(iii) There is no lattice distortion at the impurity site.

Hypotheses (ii) and (iii) are simplifications which allow us to keep the calculation within reasonable bounds; also, the value of the hyperfine constant of Mn^{2+} in calcite indicates that any covalent contribution is small.

The part of the crystalline electric field acting on the Mn^{2+} impurities in the calcite lattice, which depends on the angle ϕ with the crystal axis, can be written as

$$a_4^3(c) \mathcal{C}_4^3(\theta, \phi) + a_4^3(s) \mathcal{S}_4^3(\theta, \phi), \quad (11)$$

with⁸

$$a_4^3(c) = \frac{1}{4} \sqrt{70} \sum_i (x_i^2 - 3y_i^2)(x_i z_i) q_i / r_i^9, \quad (12a)$$

$$a_4^3(s) = \frac{1}{4} \sqrt{70} \sum_i (3x_i^2 - y_i^2)(y_i z_i) q_i / r_i^9, \quad (12b)$$

where the sum is over the ligands which, in Eqs. (12a) and (12b), are supposed to be point charges. Approximation (i) is equivalent to considering that

$$\begin{aligned} \alpha &= \frac{1}{3} \tan^{-1}(A_4^3(s)/A_4^3(c)) \\ &= \frac{1}{3} \tan^{-1}(a_4^3(s)/a_4^3(c)) = \alpha_{cf}, \end{aligned}$$

where α_{cf} is the angle between the principal axis of the electric field and the crystal axis. It follows that

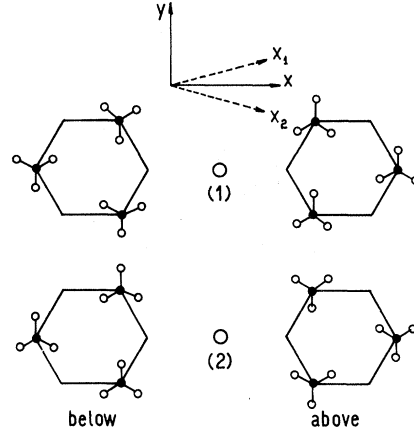


FIG. 3. Six nearest carbonates to the magnetic impurity are shown for the two inequivalent sites of Ca^{2+} in calcite. In the upper part we show with solid lines the crystal axes and with dashed lines the principal axes of the spin Hamiltonian of each site.

$$\tan 3\alpha = \frac{a_4^3(s)}{a_4^3(c)} = \frac{\sum_i [(3x_i^2 - y_i^2)(y_i z_i) / r_i^9] q_i}{\sum_i [(x_i^2 - 3y_i^2)(x_i z_i) / r_i^9] q_i}. \quad (13)$$

The sum on the numerators is only over the oxygen ligands because the calcium and carbon ions do not contribute to $a_4^3(s)$ since the point symmetry of their distribution is D_{3d} .

If point charges q_O and q_C are assigned to oxygen and carbon ions of the carbonates, with the condition

$$3q_O + q_C = -2e,$$

the values of q_O and q_C can be obtained by a simple calculation using Eq. (13) and our experimental value of α .

Considering the indeterminacy of the sign of α , two sets of values are obtained:

$$q_O = -0.82e, \quad q_C = 0.46e \quad \text{for } \alpha = -15.5^\circ;$$

$$q_O = 0.94e, \quad q_C = -4.82e \quad \text{for } \alpha = +15.5^\circ.$$

Only the first set of values is reasonable and so we obtain

$$q_O = -0.82e, \quad q_C = 0.46e, \quad \alpha = -15.5^\circ.$$

We show in Fig. 3 the position of the carbon and oxygen ions of the distorted octahedron of carbonates which surrounds the Mn^{2+} impurity; the crystalline axis and the principal axis of the spin Hamiltonian (and of the crystalline field) are also shown in Fig. 3.

The values of q_O and q_C are in good agreement with what is obtained by a simple molecular-orbital calculation of the charge distribution of the carbonate ion. As shown by Douglas and

McDaniel,¹⁸ the 24 valence-shell electrons of CO_3^{-2} are distributed in the following way:

(a) six electrons in three σ bonds formed with sp^2 hybrid carbon and oxygen orbitals; (b) two electrons in one π bond formed with P_z oxygen and carbon atomic orbitals; (c) 12 electrons in six nonbonding orbitals formed with sp^2 hybrid atomic orbitals; and (d) four electrons in two nonbonding orbitals formed with P_z atomic orbitals. The nonbonding orbitals [(c) and (d)] contain only oxygen-pure orbitals and so contribute with $-\frac{16}{3}e$ to the charge of each oxygen. Considering the electronegativities of C and O,¹⁸ the ionic character of the σ bond is about 22%; the 78% remaining charge in these bonds is shared between the carbon and oxygen. Then the six electrons in the σ bond are distributed as follows:

$$-2(0.22 + 0.39)e = -1.22e$$

in each oxygen and

$$2 \times 3 \times 0.39e = -2.34e$$

in the carbon. Of the two electrons in the π bonding orbital (b), one is in the carbon and the other is shared by the three oxygens. The total electronic charge of the valence shell of the oxygens is then $-6.88e$ and $q_O = -6.88e + 6e = -0.88e$, a value in excellent agreement with $q_O = -0.82$ calculated using our experimental data. The molecular-orbital calculation predicts also a charge $q_C = +0.64e$ at the carbon sites.

B. Angular variation of linewidths

The possible sources of the EPR linewidths of Mn^{2+} in the samples of CaCO_3 used in our experiments are the following:

(i) The spin-lattice relaxation times; This possibility was discarded because there are no important variations in the linewidths, and particularly in the angle β , when the sample is cooled to 77°K.

(ii) Random magnetic fields at the Mn^{2+} ions produced by other magnetic impurities; They also broaden the $S_z = -\frac{1}{2} \leftrightarrow -\frac{1}{2}$ transition. There is no ligand hyperfine structure since the most abundant isotopes of C, O, and Ca have $I=0$.

(iii) Random electric fields at the Mn^{2+} ions produced by crystal defects, impurities with different charge or size in the crystal,¹⁵ or a distribution of internal stresses¹⁴ due to the thermal history of the sample. These random electric fields produce no broadening of the $S_z = -\frac{1}{2} \leftrightarrow -\frac{1}{2}$ fine-structure transitions.

Equation (7) gives the angular variation of linewidths for all the trigonal point groups, but $\beta \neq 0$

only for the C_3 and S_6 groups. Our experimental value $\beta \neq 0$ indicates that the symmetry is S_6 , that is, the symmetry given by the oxygen ligands. Also, the angles α and β are equal within experimental error and so the principal axes of the angular variation of the linewidths coincide with those of the crystal field. A random distribution of the oxygen ions around their equilibrium positions would produce this effect and we conclude that the main source of broadening in our sample are random stresses in the crystal.

Very different is the result obtained for Mn^{2+} in CaWO_4 , where data on the EPR linewidths have been reported previously by us. Our data followed Eq. (8) with $\beta' = 0$ indicating as was shown in Sec. II, that the point symmetry of the source of broadening is D_{2d} , higher than the S_4 point symmetry of the crystalline field; the defects that originate the broadening are at the position of the Ca or W ions in the crystal, but not at the oxygen sites. These *point* defects are essentially different from the lattice distribution of random stresses of Mn^{2+} in CaCO_3 ; they have been studied by Mims and Guillen¹⁵ who pointed out that they can be recognized from the line shape of the inhomogeneous broadened line. This paper gives a simple way to identify the source of the broadening without measuring line shapes, a measurement which, even when a large signal-to-noise ratio of the EPR lines is obtained, is difficult to perform with the needed accuracy. Our method is not useful in the high-symmetry cases, when the crystal-line electric field is not rotated from the crystallographic axis; however, many of the low-symmetry crystals can be analyzed as in the cases of CaWO_4 and CaCO_3 .

It is of interest to note in Eq. (7) that if the term depending in the angle ϕ has the same order of magnitude as those depending only on θ , large differences between the linewidths and the height of the EPR lines would be observed for the same transition of the two nonequivalent sites. For Mn^{2+} in CaCO_3 the differences observed in our experiments are about 30% and can be explained considering the data in Fig. 2. Marshall and Reinberg¹³ observed for Fe^{3+} in CaCO_3 differences of up to a factor of 10 in the height of the EPR signal of the two nonequivalent sites. These differences were explained by an unequal population of Fe impurities at the two calcium sites in the unit cell; this is not the case observed by us for Mn^{2+} in CaCO_3 . In a forthcoming paper we will give a detailed discussion of the origin of the inhomogeneous broadening of Mn^{2+} in calcite in terms of the values of the constants of the spin-lattice interaction measured in uniaxial stress experiments.

ACKNOWLEDGMENT

The authors would like to thank Dr. Elsa Feher and Dr. Mario Passeggi for helpful suggestions. They are also grateful to Mrs. Ana Barberis for her contribution to this work.

APPENDIX A

Real combinations of the spherical harmonics can be defined by^c

$$C_n^0(\theta) = [4\pi/(2n+1)]^{1/2} Y_n^0(\theta), \quad (A1)$$

$$C_n^m(\theta, \phi) = (1/\sqrt{2}) [4\pi/(2n+1)]^{1/2} \times [Y_n^{-m} + (-1)^m Y_n^m], \quad (A2)$$

$$S_n^m(\theta, \phi) = (i/\sqrt{2}) [4\pi/(2n+1)]^{1/2} \times [Y_n^{-m} - (-1)^m Y_n^m]. \quad (A3)$$

These definitions differ from that given by Prather by a factor of $[4\pi/(2n+1)]^{1/2}$. It gives

$$C_2^0(\theta) = \frac{1}{2}(3 \cos^2 \theta - 1),$$

$$C_4^0(\theta) = \frac{1}{8}(35 \cos^4 \theta - 30 \cos^2 \theta + 3),$$

$$C_4^3(\theta, \phi) = \frac{1}{4} \sqrt{70} \sin^3 \theta \cos \theta \cos 3\phi,$$

$$S_4^3(\theta, \phi) = \frac{1}{4} \sqrt{70} \sin^3 \theta \cos \theta \sin 3\phi.$$

The transformation rules of these functions can be derived from the rotation matrices of the spherical harmonics as obtained from the tables given by Prather. Spin operators equivalent to these defined in Eqs. (A1), (A2), and (A3) could be defined. They are

$$C_2^0(S_z) = \frac{1}{2} [3S_z^2 - S(S+1)],$$

$$C_4^0(S_z) = \frac{1}{8} [35S_z^4 - 30S(S+1)S_z^2 + 25S_z^2 + 3S^2(S+1)^2 - 6S(S+1)],$$

$$C_4^3(\vec{S}) = \frac{1}{16} \sqrt{70} [S_z^3(2S_z - 3) + S_z^3(2S_z + 3)],$$

$$S_4^3(\vec{S}) = \frac{1}{16} i \sqrt{70} [S_z^3(2S_z - 3) - S_z^3(2S_z + 3)].$$

Their matrix elements between spin states with constant S could be obtained using the tables given by Hutchings¹⁹ for the Stevens spin operators. The convenience of using normalized operators comes evident when they have to be rotated to different directions of the magnetic field.

APPENDIX B

The orientation of the c crystal axis of the calcite along the quartz rod of the goniometer was performed within 1° . The position of an EPR transition is given by Eq. (6) as a function of the direction of the magnetic field.

However, due to any misalignment of the sample

$$\theta = \theta_0 + \epsilon \sin(\phi - \phi_1), \quad (B1)$$

where ϵ and ϕ_1 are the spherical angles giving the direction of the quartz rod in the crystal system of coordinates, and $\theta_0 = 60^\circ$. Equation (B1) is correct up to terms linear in ϵ . If it is replaced in Eq. (6), the following dependence is obtained for a $-\frac{5}{2} \rightarrow -\frac{3}{2}$ transition up to terms linear in ϵ (in gauss):

$$\Delta H = 433\epsilon \sin(\phi - \phi_1) + \frac{15}{32} \sqrt{210} \times [A_4^3(c) \cos 3\phi \pm A_4^3(s) \sin 3\phi], \quad (B2)$$

where

$$H = K(-\frac{3}{2}, \phi_0) + \Delta H$$

and $K(S_z, \theta)$ is obtained comparing Eqs. (4) and (5).

The least-square fit of the experimental data was done with Eq. (6) and the correction given by Eq. (B2) where ϵ , ϕ_1 , $A_4^3(c)$, and $A_4^3(s)$ are adjustable parameters. We obtain $\epsilon = 1.1^\circ$ and $\phi_1 = 141^\circ$ in agreement with the previous idea.

*Work supported in part by the Consejo Nacional de Investigaciones Científicas y Técnicas, República Argentina.

†Members of the Carrera del Investigador Científico, Consejo Nacional de Investigaciones Científicas y Técnicas, República Argentina.

¹F. K. Hurd, M. Sachs, and W. D. Hershberger, *Phys. Rev.* **93**, 373 (1954).

²C. Kikuchi, *Phys. Rev.* **100**, 1243 (1955).

³H. M. McConnell, *J. Chem. Phys.* **24**, 904 (1956).

⁴C. Kikuchi and L. M. Matarrese, *J. Chem. Phys.* **33**, 601 (1960).

⁵J. A. Hodges, S. A. Marshall, J. A. McMillan, and R. A. Serway, *J. Chem. Phys.* **49**, 2857 (1968).

⁶L. M. Matarrese, *J. Chem. Phys.* **34**, 336(L) (1961).

⁷R. A. Serway, *Phys. Rev.* **B3**, 608 (1971).

⁸J. L. Prather, *Monogr. U. S. Natl. Bur. Stand.* **19**

(1961).

⁹R. W. G. Wyckoff, *Crystal Structures* (Interscience, New York, 1949).

¹⁰G. E. Barberis and R. Calvo, *Solid State Commun.* **12**, 963 (1973).

¹¹D. Shaltiel and W. Low, *Phys. Rev.* **124**, 1062 (1961).

¹²J. S. Van Wieringen and J. G. Rensen, in *Proceedings of an International Conference in Jerusalem, 1963* (unpublished).

¹³S. A. Marshall and A. R. Reinberg, *Phys. Rev.* **132**, 134 (1963).

¹⁴E. R. Feher, *Phys. Rev.* **136**, A145 (1964).

¹⁵W. B. Mims and J. Guillen, *Phys. Rev.* **148**, 438 (1966).

¹⁶A. M. Stoneham, *Rev. Mod. Phys.* **41**, 82 (1969).

¹⁷See, for example, R. R. Sharma, T. P. Das, and R. Orbach, *Phys. Rev.* **149**, 257 (1966); **155**, 338 (1967); **171**, 378 (1968).

¹⁸B. E. Douglas and D. H. McDaniel, *Concepts and Models of Inorganic Chemistry* (Blaisdell, New York, 1965).

¹⁹M. T. Hutchings, in *Solid State Physics*, edited by F. Seitz and D. Turnbull (Academic, New York, 1964), Vol. 16.